Cardiovascular Diabetology

RESEARCH

Open Access

SGLT2 inhibitor downregulates ANGPTL4 to mitigate pathological aging of cardiomyocytes induced by type 2 diabetes

Yun Wen[1,2], Xiaofang Zhang[2,3], Han Liu[1,2], Haowen Ye[1,2], Ruxin Wang[1,2], Caixia Ma[1,2], Tianqi Duo[2], Jiaxin Wang[1,2], Xian Yang[1,2], Meixin Yu[1,2], Ying Wang[1,2], Liangyan Wu[1], Yongting Zhao[1] and Lihong Wang[1,2*]

Abstract

Background Senescence is recognized as a principal risk factor for cardiovascular diseases, with a significant association between the senescence of cardiomyocytes and inferior cardiac function. Furthermore, type 2 diabetes exacerbates this aging process. Sodium-glucose co-transporter 2 inhibitor (SGLT2i) has well-established cardiovascular benefits and, in recent years, has been posited to possess anti-aging properties. However, there are no reported data on their improvement of cardiomyocytes function through the alleviation of aging. Consequently, our study aims to investigate the mechanism by which SGLT2i exerts anti-aging and protective effects at the cardiac level through its action on the FOXO1-ANGPTL4 pathway.

Methods To elucidate the underlying functions and mechanisms, we established both in vivo and in vitro disease models, utilizing mice with diabetic cardiomyopathy (DCM) induced by type 2 diabetes mellitus (T2DM) through high-fat diet combined with streptozotocin (STZ) administration, and AC16 human cardiomyocyte cell subjected to stimulation with high glucose (HG) and palmitic acid (PA). These models were employed to assess the changes in the senescence phenotype of cardiomyocytes and cardiac function following treatment with SGLT2i. Concurrently, we identified ANGPTL4, a key factor contributing to senescence in DCM, using RNA sequencing (RNA-seq) technology and bioinformatics methods. We further clarified ANGPTL4 role in promoting pathological aging of cardiomyocytes induced by hyperglycemia and hyperlipidemia through knockdown and overexpression of the factor, as well as analyzed the impact of SGLT2i intervention on ANGPTL4 expression. Additionally, we utilized chromatin immunoprecipitation followed by quantitative real-time PCR (ChIP-qPCR) to confirm that FOXO1 is essential for the transcriptional activation of ANGPTL4.

Results The therapeutic intervention with SGLT2i alleviated the senescence phenotype in cardiomyocytes of the DCM mouse model constructed by high-fat feeding combined with STZ, as well as in the AC16 model stimulated by HG and PA, while also improving cardiac function in DCM mice. We observed that the knockdown of ANGPTL4, a key senescence-promoting factor in DCM identified through RNA-seq technology and bioinformatics, mitigated the

Yun Wen is the first author, Xiaofang Zhang and Han Liu are the co-first authors.

*Correspondence:
Lihong Wang
nd6688@163.com

Full list of author information is available at the end of the article

senescence of cardiomyocytes, whereas overexpression of ANGPTL4 exacerbated it. Moreover, SGLT2i improved the senescence phenotype by suppressing the overexpression of ANGPTL4. In fact, we discovered that SGLT2i exert their effects by regulating the upstream transcription factor FOXO1 of ANGPTL4. Under conditions of hyperglycemia and hyperlipidemia, compared to the control group without FOXO1, the overexpression of FOXO1 in conjunction with SGLT2i intervention significantly reduced both ANGPTL4 mRNA and protein levels. This suggests that the FOXO1-ANGPTL4 axis may be a potential target for the cardioprotective effects of SGLT2i.

Conclusions Collectively, our study demonstrates that SGLT2i ameliorate the pathological aging of cardiomyocytes induced by a high glucose and high fat metabolic milieu by regulating the interaction between FOXO1 and ANGPTL4, thereby suppressing the transcriptional synthesis of the latter, and consequently restoring cardiac function.

Graphical abstract

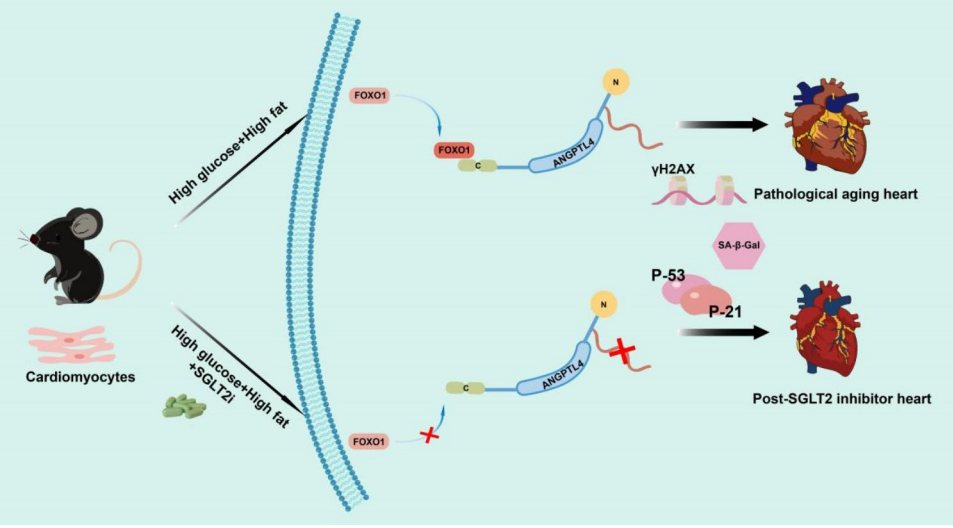

Keywords SGLT2i, Diabetic cardiomyopathy, Cellular senescence, ANGPTL4, FOXO1

Background

Cardiovascular diseases are a leading cause of mortality, and with the acceleration of population aging, senescence has emerged as a significant risk factor for cardiovascular conditions [1]. Studies have confirmed that the rate of aging in diabetic patients is approximately a decade faster than in the general population, a phenomenon that may be attributed to diabetes-associated "accelerated aging" [2, 3]. Cardiomyocytes have been identified as highly sensitive to aging [4], with senescent cardiomyocytes undergoing a precipitous loss in cell number and profound alterations in their transcriptional profiles. Clinical observations also indicate a close association between the accumulation of senescent cells in the heart and poorer cardiac function [5].

Cellular senescence is one of the primary causes of aging and age-related diseases. In multicellular organisms, the aging of the organism does not equate to the aging of all cells, however, cellular senescence is closely related to the aging of the organism. The accumulation of senescent cells in tissues can ultimately accelerate the progression of age-related diseases, such as diabetes and cardiac disease [6]. A series of changes that occur during cellular senescence, including functional disorders and DNA damage, are observed not only in the cells of the elderly but also in cells subjected to continuous damage by various harmful factors, including excessive caloric intake mediated by high glucose and high fat. Research has shown that excessive caloric intake in young mice induces adipocyte senescence through the activation of p53 and p21 by reactive oxygen species (ROS) [7], potentially leading to insulin resistance and reduced glucose tolerance. In contrast, mice and humans under caloric restriction exhibit lower levels of senescence markers [8]. For the heart, excess energy can induce senescence, reduce the heart's stress tolerance, and accelerate cardiac aging [9, 10]. Moreover, once cardiomyocytes damage and senescence are triggered, even stringent control of blood glucose and lipid levels cannot reverse the progression of the damage. In patients with type 2 diabetes, myocardial diseases that cannot be attributed to hypertensive heart disease, coronary atherosclerotic heart disease, or other cardiac pathologies are termed diabetic cardiomyopathy (DCM) [11]. DCM can lead to heart failure,

arrhythmias, and sudden death, with a high fat and high glucose environment being the core factor in its pathogenesis [12]. Although an increasing number of studies have investigated the role of cellular senescence in diabetic cardiomyopathy, the specific mechanisms remain unclear, particularly the knowledge gap regarding potential therapeutic drugs targeting cellular senescence and their mechanisms.

Furthermore, the potential of SGLT2i to intervene in the terminal events of cardiovascular disease, their progression, and readmission rates has been demonstrated through extensive clinical trial data, such as the CANVAS, EMPA-REG, and DAPA-HF trials [13–15]. In the FDA's ranking of clinical potential for anti-aging drugs, SGLT2i are considered superior to other medications like rapamycin, metformin, and resveratrol, showing significant anti-aging potential in both experimental and clinical applications [16]. A multitude of basic experiments have proven that in both in vivo and in vitro injury models, SGLT2i are not limited to improving heart function by inhibiting renal tubular SGLT2 receptors, increasing urinary glucose excretion, and promoting osmotic diuresis. SGLT2i can directly affect pathways such as NRF2/ARE and hypoxia-inducible factor 1α [17, 18], thereby exerting a direct protective effect on the heart. However, the ability of SGLT2i to induce cardioprotection by improving cellular senescence has not yet been studied.

In our study, to better clarify the beneficial characteristics of SGLT2i in cardiovascular protection, we used both high-fat feeding combined with STZ to induce DCM mice and HG+PA to stimulate AC16 human cardiomyocyte cell as in vivo and in vitro disease models, respectively. We assessed the impact of SGLT2 inhibitors on cellular senescence induced by high fat and high glucose.

Methods

Mouse model of DCM and drug administration

Male C57BL/6J mice (6-8weeks old, 22±2 g) were purchased from Beijing Vital River Laboratory Animal Technology Co., Ltd. After one week of acclimatization under specific pathogen-free (SPF) laboratory conditions, the mice were randomly grouped. The diet of the modeling group was switched to a 60% high-fat diet (HFD). After 12weeks, the mice in the model group received a single intraperitoneal injection of Streptozotocin (STZ) at a dose of 50 mg/kg. Five days post-STZ induction, tail vein blood from each group of mice was collected to measure fasting blood glucose levels. Mice with fasting blood glucose levels above 16.7mmol/L for three consecutive days were considered successfully modeled. After successful modeling, Empagliflozin (EMPA) was administered via gavage at a dose of 10 mg/kg/day, given between 9 and 10 AM, for a total of 10 weeks [19–21]. Two weeks after the end of the drug administration, changes in cardiac function in each group of mice were detected using a small animal ultrasound imaging system.

Cell culture

The AC16 human cardiomyocyte cell line. According to the manufacturer's instructions, mycoplasma contamination of this cell line was tested and identified as negative. Cells were cultured in DMEM medium (purchased from Corning Inc., USA) containing 12.5% fetal bovine serum (FBS) (purchased from Corning Inc., USA), and 1% antibiotic penicillin-streptomycin (purchased from Gibco, USA). The cell line was maintained at 37 °C and 5% carbon dioxide in an incubator. Cells were grown between passages 5 to 7, and experiments were repeated three times. AC16 cells were exposed to 33.3mmol/L D-glucose and treated with 0.5μM EMPA (purchased from MCE Company, USA). Cells exposed to normal glucose (NG) concentration (4.5mmol/L) were considered the control group and were cultured for 48 h.

Heart tissue and AC16 cells staining

HE staining

Left ventricular tissue from mice was fixed, paraffin-embedded, sectioned, deparaffinized, and hydrated. Sections were then stained with hematoxylin solution, rinsed, differentiated, and subsequently stained with eosin solution, followed by dehydration, clearing, and the tissue sections were visualized and photographed using a StrataFAXS P-S automated slide scanning system (TissueGnostics, Austria).

Masson's trichrome staining

Sections of left ventricular tissue were deparaffinized and stained with Weigert's iron hematoxylin, differentiated with acidic ethanol, and then rinsed. The sections were immediately blued with Masson's blue solution, rinsed, and stained with fuchsin-acidic solution followed by washing with weak acid and phosphomolybdic acid solution. After staining with aniline blue and washing with weak acid solution, the sections were dehydrated with ethanol, cleared with xylene, and the tissue sections were visualized and photographed using a StrataFAXS P-S automated slide scanning system (TissueGnostics, Austria).

γ-H2AX immunofluorescence staining

Sections of left ventricular tissue and AC16 cells were deparaffinized and hydrated. According to the instructions of the kit (purchased from Beyond Biotechnology Co., Ltd., China), non-specific antigen sites were blocked with serum working solution; specific primary antibodies and fluorescent secondary antibodies were incubated, and after incubation in the dark, the cells were stained with nuclear staining solution (DAPI) at room

temperature. After cleaning the liquid around the tissue, an appropriate amount of anti-fluorescence quenching solution was added for mounting, and the samples were observed and photographed using a full-spectrum fluorescence lifetime confocal imaging system (Leica Microsystems, Germany).

Cellular senescence β-Gal staining

AC16 cells were fixed with β-Gal staining fixative at room temperature after growth on slides. After washing off the fixative, staining solution was prepared according to the instructions of the kit (purchased from Beyond Biotechnology Co., Ltd., China), and the cells were incubated overnight at 37 °C. The stained cells were observed and counted under a standard optical microscope (Leica Microsystems, Germany).

ELISA method for detecting SASP levels in myocardial tissue of mice

An appropriate amount of myocardial tissue was homogenized in physiological saline using an ultrasonic homogenizer. The homogenate was centrifuged at 4 °C and 4000 g for 15 min, and the supernatant was collected. The levels of senescence-associated secretory phenotype (SASP) factors, include interleukin-1β (IL-1β) and interleukin-6 (IL-6), were determined by measuring the absorbance (A) at 450 nm using an ELISA kit (purchased from Hangzhou Union Biotechnology Co., Ltd.), and the levels were calculated based on the A value and the standard curve.

Protein extraction and western blotting

An appropriate amount of myocardial tissue and cell protein lysate was added to RIPA lysis buffer, sonicated to promote lysis, and centrifuged at 4 °C and 12,000 g for 20 min. The supernatant was collected, and protein content was measured using a BCA assay kit. Thirty micrograms of protein were added to 5×loading buffer and heated in a metal bath for 10 min. Proteins were separated by 12% SDS-PAGE electrophoresis and transferred onto PVDF membranes using wet transfer methods. The membranes were blocked with 5% skim milk at room temperature for 1.5 h, washed three times with TBST, and then incubated with primary antibodies against P53 (1∶1000), P21 (1∶1000), ANGPTL4 (1∶1000) and ACTIN (1∶5000) overnight at 4 °C. After four washes with TBST, HRP-conjugated goat anti-rabbit IgG secondary antibodies (1∶5000) and anti-mouse IgG secondary antibodies (1∶5000) were added and incubated at room temperature for 1 h. The membranes were washed three times with TBST, developed with ECL reagent, and visualized using a highly sensitive multifunctional imaging system. Densitometry analysis was performed using Image J software.

RNA extraction and quantitative real-time PCR

Total RNA was isolated and purified using phenol and chloroform. cDNA was synthesized from 1 μg of total RNA using the QuantiTect Reverse Transcription Kit (TOYOBO Corporation, Japan). DNA amplification reactions were conducted using a PCR amplification kit (PerfectStart® Green qPCR SuperMix).

Primer sequences:
ANGPTL4 (Human): forward 5′–3′ATGGAGGCTGG ACAGTAATTCAG.
reverse 5′–3′GCTATGCACCTTCTCCAGACC;
ANGPTL4 (Mouse): forward 5′–3′CCCAGCAGCAGA GATACCTATC.
reverse 5′–3′GGTCATCTTGGGAAGCCTCTTTC;
FOXO1 (Human): forward 5′–3′TTGCCCAACCAAA GCTTCCC.
reverse 5′–3′TTGCTGCCAAGTCTGACGAAA;
FOXO1 (Mouse): forward 5′–3′CTTCCCACACAGTG TCAAGACTA.
reverse 5′–3′GCCAAGTCTGAGGAAAGGAGAAA;

For each amplification cycle, a threshold cycle (Ct) value was obtained, and the ΔCt, which is the difference in Ct values between the target mRNA and the housekeeping gene mRNA (β-Actin), was calculated. The fold increase in mRNA expression relative to the control group was determined using the $2-\Delta\Delta Ct$ method. Bar graphs reported the genes from three independent experiments, with the control group set to a value of 1.

Transfection with siRNA and overexpression plasmids

siRNA plasmids for interference were designed and synthesized by Beijing Qingke Biotechnology Co., Ltd., while overexpression plasmids were extracted and purified by Shandong Wei Zhen Biotechnology Co., Ltd. When the density of AC16 cells reached 60-80%, transfection was carried out. After preparing the transfection solution, Opti-MEM serum-free medium was used for transfection. The medium containing the transfection solution was removed after 8 h, and replaced with complete growth medium. After a 48 h incubation, the cells were treated with high glucose and PA, followed by detection of mRNA and protein levels.

Chromatin immunoprecipitation followed by quantitative real-time PCR (ChIP-qPCR)

ChIP chromatin was prepared using the truChIP Chromatin Shearing Kit (Covaris, USA). AC16 cells were cross-linked with freshly prepared 11.1% formaldehyde for 10 min, and primary mouse cardiomyocytes for 5 min, and the cross-linking was stopped at room temperature by adding 300 μl of Quenching Buffer E. Subsequently, according to the kit instructions, the nuclei were

prepared and transferred to AFA tubes for sonication in a Covaris sonicator to shear the chromatin, and the shearing efficiency of different cells was detected by DNA electrophoresis and Western blotting. The sheared chromatin was diluted at a ratio of 1:1 with Covaris 2X IP Dilution Buffer (10 µl 2X IP Dilution Buffer + 20 µl 5X PIC), centrifuged, and the supernatant was taken for downstream IP detection. The SimpleChIP® Plus Sonication ChIP Kit 4 C and RT Reagents kit from CST was used for the ChIP assay. Diluted chromatin samples (500 µl) were incubated with 10 µl of FOXO1 antibody overnight at 4 °C with shaking. The next day, magnetic beads were added and incubated at 4 °C with shaking, followed by washing, and each IP sample was eluted with 1X ChIP elution buffer at 65 °C for 30 min with shaking. The cross-linking was reversed, and DNA was purified using a centrifugal column. The ChIP experiment was analyzed by qPCR using specific primers. The recovery of ChIP and DNA was calculated as IP/Input%.

Sequence:
ANGPTL4-FOXO1 (Human): forward 5′–3′gcc tca ctc agt act tcc ttt gtc.
reverse 5′–3′aag ttc tca ggc agg tgg aga tac;
ANGPTL4-FOXO1 (Mouse): forward 5′–3′tga caa ggt ctt ctt cct gga tgg.
reverse 5′–3′gaa gca att gga gga agc tct gtg;

Bioinformatics analysis

R software (version 4.2.1) was utilized for the normalization and probe annotation of RNA-seq data. Differential expression analysis was conducted using the "limma" package in R, and the results were visualized using volcano plots and heatmaps generated by the "ggplot2" and "pheatmap" packages, respectively. Genes with a fold change (FC) greater than 2 in log2 scale and a p-value less than 0.05 were considered differentially expressed genes (DEGs). The log2 (FC) values were used to perform Gene Set Enrichment Analysis (GSEA) with the "clusterprofiler" package, and pathways with a normalized enrichment score (NES) greater than 2, a false discovery rate (FDR) less than 0.25, and a p-value less than 0.05 were selected. Additionally, reactome pathway enrichment analysis was performed on the DEGs to assess their functions, locations, or pathways, and the results were visualized using bubble charts. Finally, an intersection with the DEGs and the CellAge database was conducted, and a Venn diagram was created using the online tool at http://bioinformatics.psb.ugent.be/webtools/Venn/ to visualize the overlap.

Data analysis

Experimental data were statistically analyzed and graphed using GraphPad Prism software version 8.0. Comparisons between two samples were performed using the two-sample independent t-test, while multiple group data were assessed using one-way analysis of variance (ANOVA). A p-value less than 0.05 was considered to indicate statistical significance.

Results

SGLT2i improves cardiac function and cardiomyocytes senescence in mice with DCM

To characterize features in DCM mice, we utilized a high-fat diet combined with STZ to construct the model in C57BL/6J mice (Fig. 1A). A significant decrease in ejection fraction (EF) and fractional shortening (FS) values was observed in DCM mice compared to the wild-type (WT) group ($p < 0.05$ vs. WT) (Fig. 1B-D). Cardiomyocytes disarray, increased cell spacing, and severe myocardial fibrosis were evident, indicating successful model establishment. Additionally, we selected some DCM model mice for treatment with EMPA via gavage, and compared to the untreated DCM model group and the DCM + NS group (saline), the DCM + SGLT2i (EMPA) group showed alleviation of cardiac dysfunction (Fig. 1B-D), reduced cardiomyocytes disarray, narrowed cell spacing, and reduced myocardial fibrosis (Fig. 1E).

Furthermore, we examined several key characteristics of myocardial tissue senescence, including p53 and p21, SASP, and phosphorylated histone 2AX (γ-H2AX) to demonstrate the impact of SGLT2i treatment on myocardial senescence. Compared to the WT group, the untreated DCM model group and the DCM + NS group showed increased levels of senescence-associated indicators (Fig. 1F-L) ($p < 0.05$ vs. WT), while the DCM + SGLT2i group decreased serum levels of IL-6 and IL-1β (Fig. 1F, G), exhibited reduced expression of p53 and p21 proteins (Fig. 1H-J), and reduced γ-H2AX fluorescence staining indicating less DNA damage (Fig. 1K, L) ($p < 0.05$ vs. DCM/DCM + NS).

These results suggest that SGLT2i(EMPA) can improve cardiac function and reduce senescence in the DCM animal model induced by type 2 diabetes mellitus.

Impact of SGLT2i on Senescence in Cardiomyocytes exposed to HG + PA

Compared to cells exposed to low glucose (LG) concentrations, cells exposed to HG + PA demonstrated more pronounced cellular senescence characteristics. These included increased levels of p53 and p21 proteins (Fig. 2A-D), elevated activity of senescence-associated β-galactosidase (β-Gal) (Fig. 2E and F), and a significant increase in green fluorescence of γ-H2AX (Fig. 2G and H) ($p < 0.05$ vs. LG).

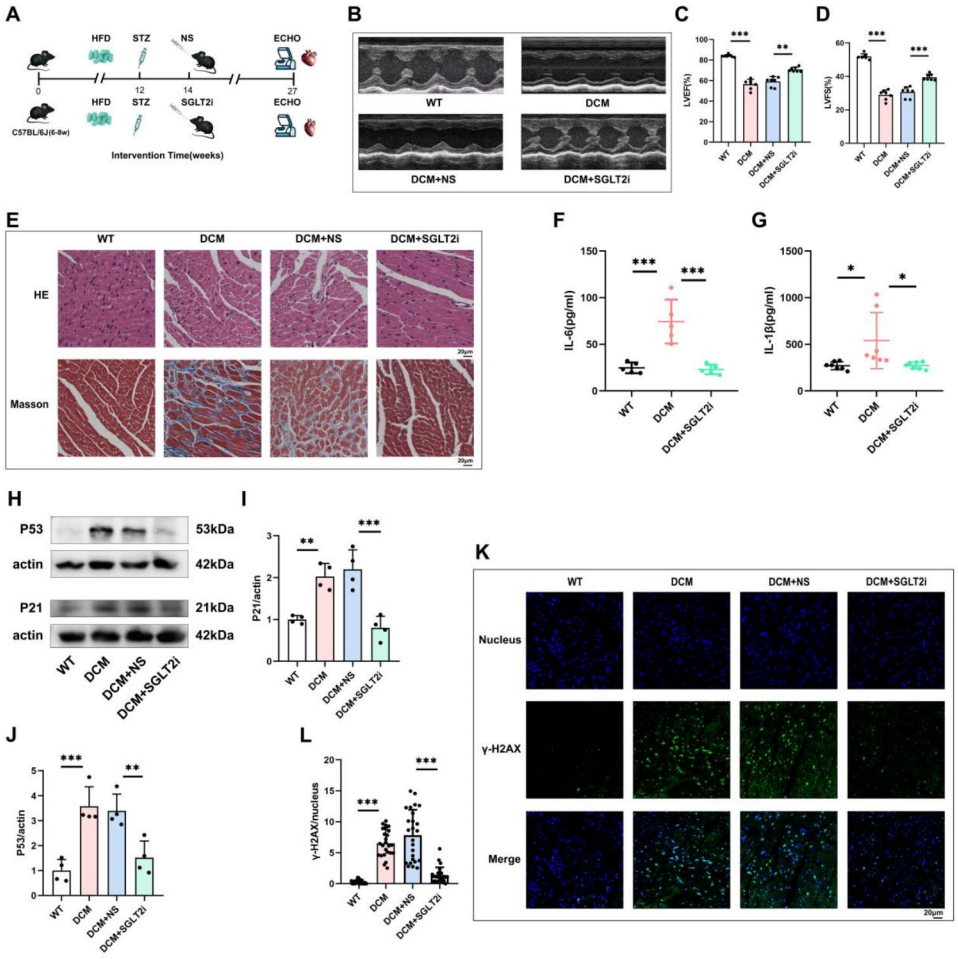

Fig. 1 SGLT2 Inhibitors Ameliorate Cardiac Dysfunction and Cellular Senescence in DCM Mice Induced by High-Fat Diet and STZ. **A** Treatment with SGLT2 inhibitors in DCM mice model induced by a high-fat diet and STZ. **B** Representative echocardiographic images of mouse hearts. **C** and **D** Levels of left ventricular ejection fraction (LVEF) and left ventricular fractional shortening (LVFS). **E** Representative H&E staining (top) and Masson's trichrome staining (bottom) of cardiac sections; scale bar, 20 mm. **F** and **G** Expression levels of IL-6 and IL-1β in serum detected by ELISA. **H**–**J** Detection of P53 and P21 by Western blotting. **K** and **L** Immunofluorescent staining of γ-H2AX (green) in mouse hearts; scale bar, 20 mm. Data are presented as mean ± SEM; *$p < 0.05$ **$p < 0.01$, ***$p < 0.001$

Treatment with EMPA markedly improved the aforementioned cellular senescence characteristics (Fig. 2) ($p < 0.05$ vs. HG+PA/HG+PA+DMSO). These results indicate that high glucose and high fat can induce cellular senescence in cardiomyocytes, and treatment with EMPA can suppress this process.

RNA-Seq and bioinformatics analysis predicted candidate gene

Associated with cardiac aging in DCM we employed RNA-seq to analyze the transcriptome of cardiac tissue from WT and DCM mice, studying the differential gene expression in the cardiac environment induced by T2DM. After filtering, alignment, and quality control of the RNA-seq output, we obtained a list of transcripts with the highest signal intensity. Using the "limma" package in R, we identified differentially expressed genes, with 470 significantly upregulated genes and 409 significantly downregulated genes in the DCM group. The results of DEGs were visualized as volcano plots and heatmaps (Fig. 3A and B). To further understand the signaling pathways involved, we performed GSEA on all genes after differential analysis, sorted by Log2 (FC) value (Fig. 4). The results showed enrichment in cellular aging-related pathways such as DNA damage, Telomere stress Induced Senescence, and SASP. Additionally, reactome pathway enrichment analysis on DEGs was conducted, and after visualization with bubble charts, the results were similar to those of GSEA, showing enrichment in aging-related pathways like recombination at telomeres, DNA Damage/Telomere Stress Induced Senescence and SASP (Fig. 3C). Subsequently, we obtained 494 aging-related genes from the CellAge database and intersected them with DEGs, identifying 20 common differential genes displayed in

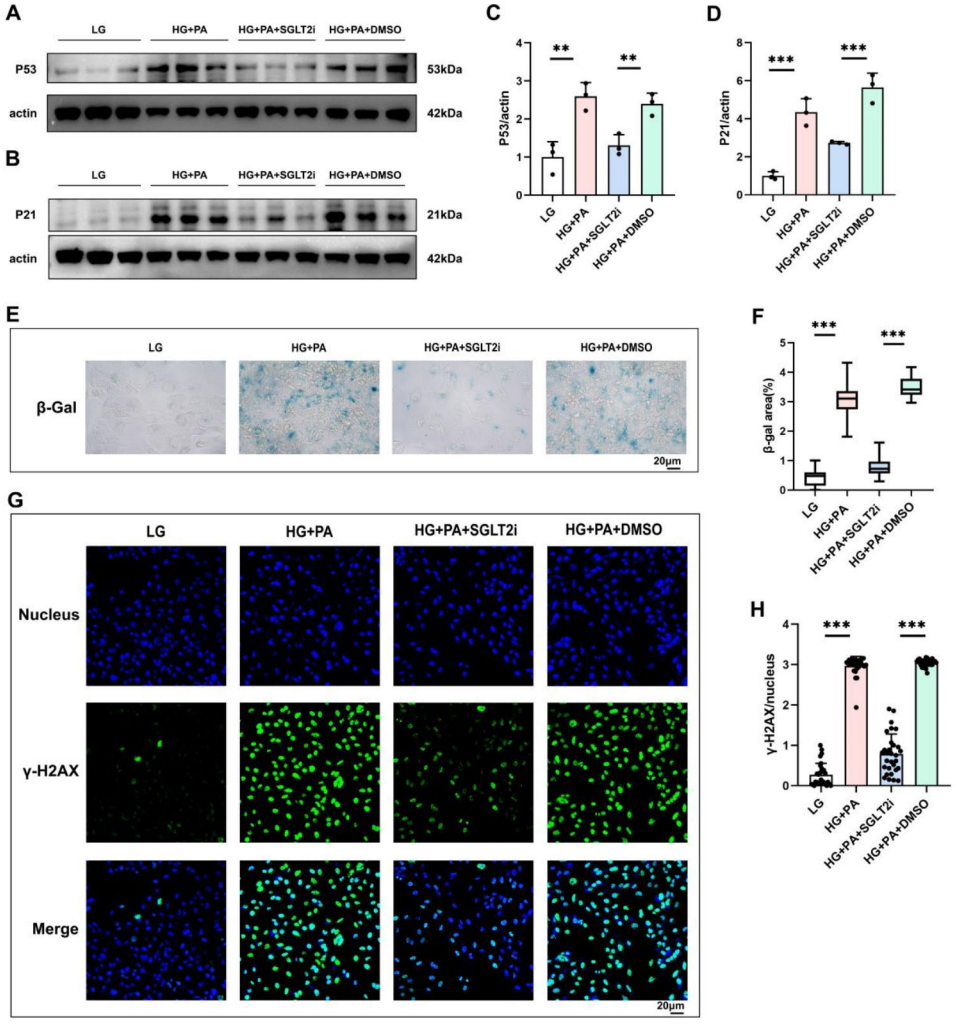

Fig. 2 SGLT2 Inhibitors Mitigate Cellular Senescence in Human Ventricular Cardiomyocyte cell (AC16) Exposed to High Glucose(HG)and Palmitic Acid(PA). **A**–**D** AC16 cells were treated with LG(1mmol/L) and HG(33.3mmol/L) + PA(100μM) for 48 h, followed by incubation with SGLT2 inhibitors (0.5μM) for an additional 48 h. P53 and P21 proteins in cell lysates were detected by Western blotting. **E** and **F** β-galactosidase staining(β-gal) of AC16 cells; scale bar, 20 mm. **G** and **H** Immunofluorescent staining of γ-H2AX (green) in AC16 cells; scale bar, 20 mm. Data are presented as mean ± SEM; *$p < 0.05$ **$p < 0.01$, ***$p < 0.001$

a Venn diagram (Fig. 3D). Among the remaining candidates, ANGPTL4 appeared to be the most promising. We detected the expression of ANGPTL4 in both in vivo and in vitro models, and compared to the WT group, the protein levels of ANGPTL4 were increased in the DCM group (figure S1 D-F). In the HG + PA-stimulated AC16 cardiomyocyte cell group, the mRNA and protein levels of ANGPTL4 were both elevated compared to the LG group (figure S1 G-I). Additionally, following treatment with STLG2i, both mRNA and protein expression levels of ANGPTL4 were found to be reduced, in both in vivo and in vitro settings (figure S1 D-I). The outcomes of the experiments aligned with the findings from the bioinformatics analysis.

Knockdown of ANGPTL4 reduces high glucose and high Fat-Induced cardiomyocytes senescence

We examined the role of ANGPTL4 knockdown in high glucose and PA-stimulated AC16 cardiomyocyte cell in vitro. Utilizing the Xtreme transfection siRNA, we observed a significant reduction in both mRNA and protein levels of ANGPTL4 after knockdown (Figure S2A-C).

Compared to the control high glucose and high fat group with an empty vector, the cellular senescence indicators in the ANGPTL4 knockdown group were improved. Expression levels of P53 and P21 proteins were decreased (Fig. 5A-D), β-Gal staining activity was reduced (Fig. 5E and F), and γ-H2AX immunofluorescence staining showed a decrease in the number of green fluorescent foci (Fig. 5G and H). These differences were

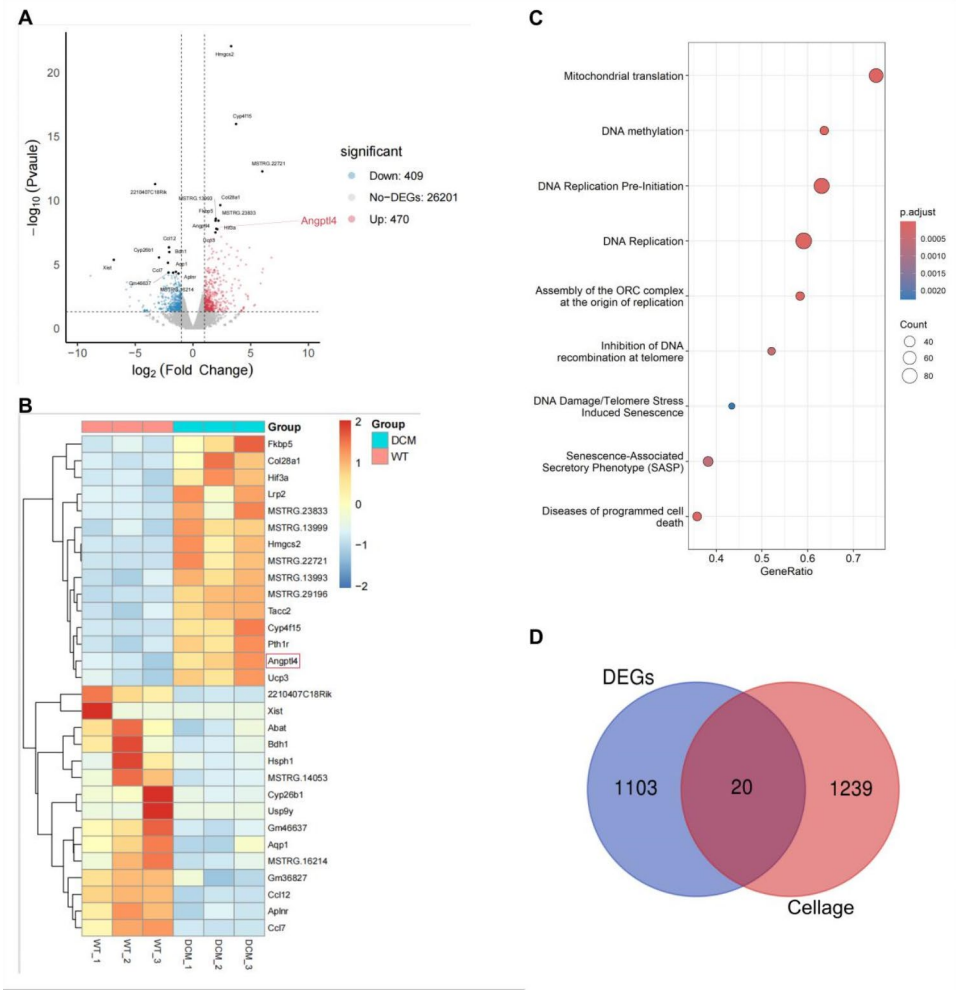

Fig. 3 Different Expression Genes (DEGs) in Cardiac Muscle Tissue from DCM Mice and WT Mice were Tested by RNA-Sequence Analysis ($n=3$). **A** and **B** Volcano plots and heatmaps display the normalized gene expression values from RNA-seq of myocardium in DCM and WT mice. **C** Functional enrichment analysis of DEGs in myocardium of DCM and WT mice. **D** Venn diagrams of overlapping genes between RNA-sequence analysis data and the CellAge database, including 20genes: ANGPTL4,CENPQ, LSM3,IMPA2,FKBP5,PSRC1,UBE2T, DIO2,CXCL10,MX1,IFIT3,E2F8,MYBL2,IFIT2,CDCA7, IS–G15,SYT1,IFIT1,CCNG1,EEF1E1

not significant in the low glucose group, indicating that ANGPTL4 knockdown can attenuate the senescence phenotype in AC16 cardiomyocyte cell induced by HG+PA.

Overexpression of ANGPTL4 exacerbates high glucose and PA-induced cardiomyocyte senescence while SGLT2i can ameliorate this effect

We used the Lipo2000 transfection overexpression plasmid, and after overexpressing ANGPTL4 in AC16 cardiomyocyte cell, both mRNA and protein levels were significantly increased (Figure S2 D-F), indicating the effectiveness of the overexpression plasmid.

Compared to the negative control group, the HG+PA group with overexpressed ANGPTL4 showed significantly increased expression levels of P53 and P21 proteins (Fig. 6A-D), elevated β-Gal staining activity (Fig. 6E and F), and an increase in green fluorescent foci in γ-H2AX immunofluorescence staining (Fig. 6G and H). These differences were not significant in the low glucose group.

To verify whether SGLT2i could ameliorate the senescence phenotype of cardiomyocytes by suppressing ANGPTL4, we subjected AC16 cardiomyocyte cell, which overexpress ANGPTL4 and were exposed to a high-glucose and PA environment, to SGLT2i intervention. Compared to the control cells with empty vector ANGPTL4 under the same high-glucose and high-fat conditions, the overexpressing cells showed a decrease in P53 and P21 protein expression levels (Fig. 7A-D), reduced β-Gal staining activity (Fig. 7E and F), and a reduction in the number of green fluorescent foci in γ-H2AX immunofluorescence staining (Fig. 7G and H), and the cellular senescence indicators were improved.

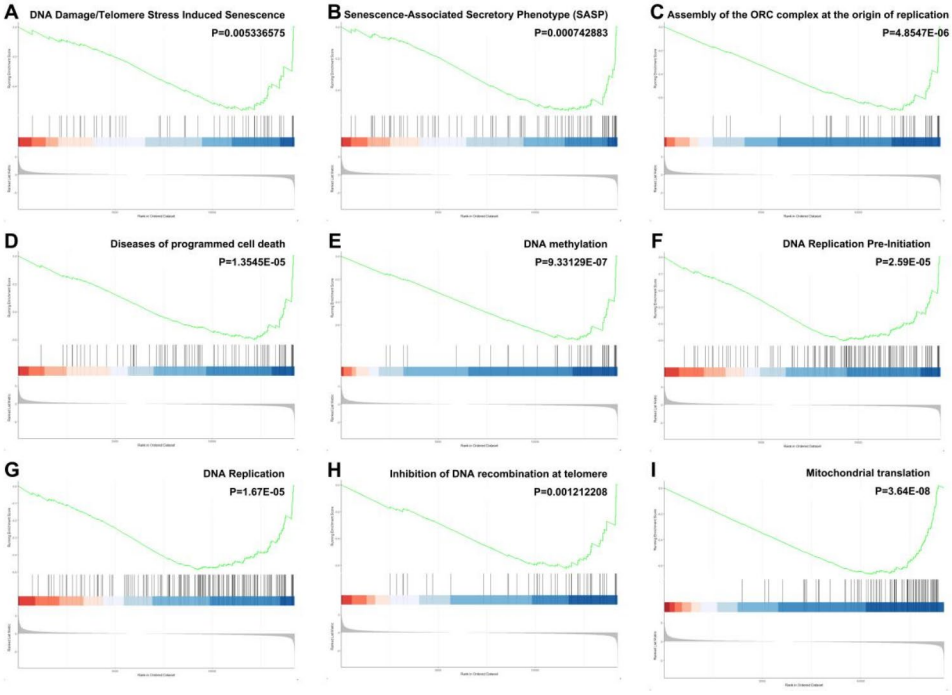

Fig. 4 Enrichment analyses using gene set enrichment analysis (GSEA)of RNA-sequence analysis. **A** DNA damage/telomere stress induced senescence. **B** Senescence-associated secretory phenotype (SASP). **C** Assembly of the oRC complex at the origin of replication. **D** Diseases of programmed cell death. **E** DNA methylation. **F** DNA Replication Pre-Initiation. **G** DNA Replication. **H** Inhibition of DNA recombination at telomere. **I** Mitochondrial translation

SGLT2i suppresses the transcription of ANGPTL4 by reducing Cardiomyocyte FOXO1

To clarify how SGLT2i suppresses the transcription of ANGPTL4 and exerts its therapeutic effect, we predicted the upstream transcription factors of ANGPTL4 using online databases (NCBI and JASPAR). Sequence alignment in the JASPAR database revealed the highest correlation coefficient between FOXO1 and the promoter region of ANGPTL4 (Fig. 8A). Knockdown of FOXO1 significantly reduced the mRNA and protein expression levels of both FOXO1 and ANGPTL4 (Fig. 8B-D), while overexpression of FOXO1 increased their levels (Fig. 8E-G).

At the same time, we overexpressed FOXO1 in AC16 cardiomyocyte cell induced by glucose and fat toxicity and combined it with SGLT2i intervention to detect the expression levels of ANGPTL4 in each group. The results showed that the expression levels of ANGPTL4 mRNA and protein decreased with SGLT2i intervention. Compared with the FOXO1 empty vector group, the group with overexpressed FOXO1 combined with SGLT2i also showed decreased levels of ANGPTL4 mRNA and protein, indicating that under conditions of high glucose and PA, SGLT2i suppresses the transcription of ANGPTL4 through FOXO1 (Fig. 8H-J).

Additionally, chromatin immunoprecipitation experiments showed that compared to the negative control group, the expression levels of the binding fragments between the ANGPTL4 promoter and FOXO1 in both AC16 cells (Fig. 8K) and primary mouse cardiomyocytes (Fig. 8L) were significantly increased, further confirming this fragment as the binding site for ANGPTL4 and FOXO1.

Discussion

Chronic hyperglycemia and hyperlipidemia in T2DM induce a pathological state that accelerates DNA damage, leading to an accelerated accumulation of senescent cells in the heart [3]. This exacerbates heart dysfunction and affects disease outcomes. In our study, we have uncovered a novel therapeutic mechanism by which SGLT2i targets cellular senescence. SGLT2, a glucose-sodium transporter located in the proximal renal tubules, was initially marketed as an antidiabetic drug by promoting glucose excretion in the urine to lower blood glucose levels. Subsequent clinical studies have shown its efficacy in heart failure, leading to an expansion of its indications [22]. However, the cardioprotective mechanisms of SGLT2i remain unclear, and we propose that their mechanism of action may include direct improvement of cardiomyocytes senescence. In a series of investigations [23], SGLT2i have been reported to induce a net caloric deficit, mimicking a fasting-like metabolic profile and triggering nutrient-deprivation pathways. These pathways may exert a variety of cardioprotective effects by activating the AMPK/SIRT1/PGC-1α [24] cascade or by inhibiting

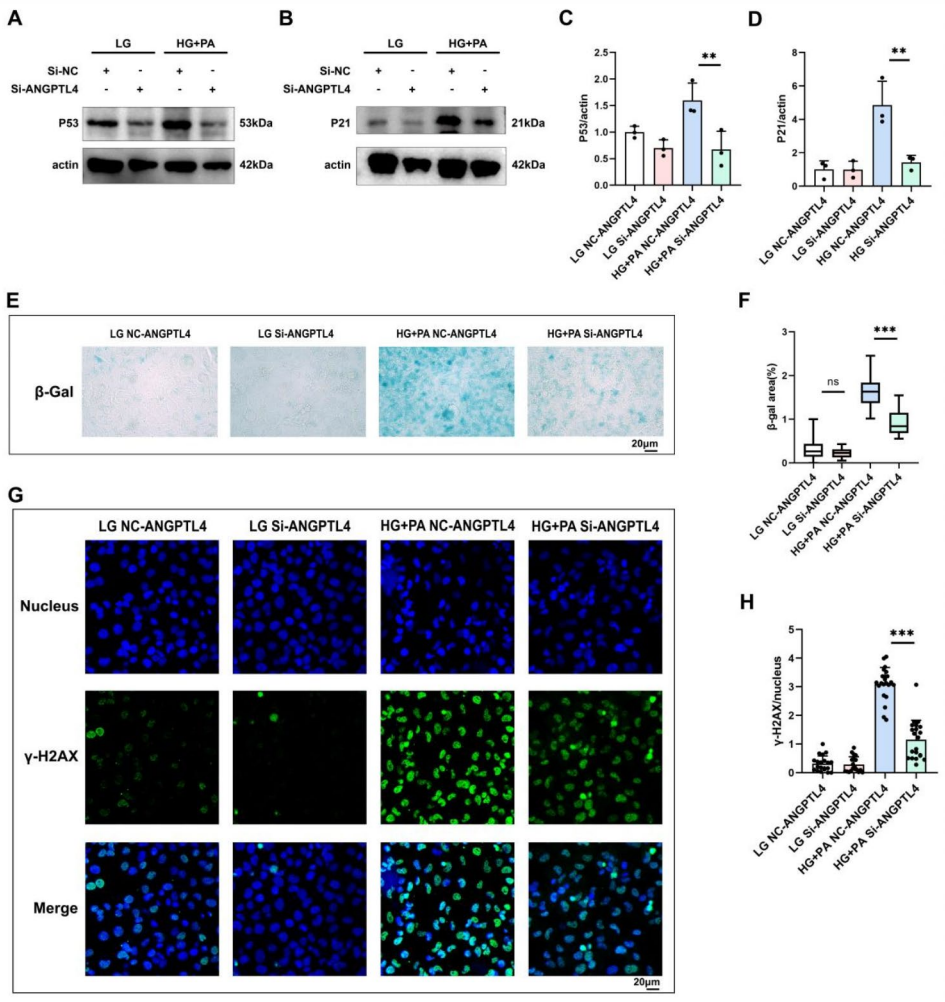

Fig. 5 Knockdown of ANGPTL4 alleviates HG+PA-Induced cellular senescence in cardiomyocytes. (**A**-**D**) P53 and P21 proteins in cell lysates were detected by Western blotting. (**E** and **F**) β-gal staining of treated AC16 cells; scale bar, 20 mm. (**G** and **H**) Immunofluorescent staining of γ-H2AX (green) in treated AC16 cells; scale bar, 20 mm. Data are presented as mean ± SEM; *$p < 0.05$ **$p < 0.01$, ***$p < 0.001$

the FOXO signaling pathway [25]. Concurrently, the role of energy intake restriction in mitigating age-related diseases and extending lifespan has been well established [26, 27]. In our study, using both in vivo and in vitro disease models of T2DM-induced DCM and high glucose and palmitic acid-stimulated AC16 cardiomyocyte cell, we observed that several key characteristics of cellular senescence, includingp53 and p21, γ-H2AX, SASP and senescence-associated β-galactosidase (β-Gal) activity, were significantly downregulated following SGLT2i intervention, along with improved cardiac function in treated mice. These findings are consistent with current research, as the accelerated accumulation of senescent cells in tissues has been reported in diabetes and heart failure, and SGLT2i can eliminate senescent cells [28, 29].

By assessing the changes in the myocardial tissue transcriptome of DCM mice and using bioinformatics for prediction, we identified ANGPTL4 as a candidate molecule associated with aging. Numerous genetic studies have demonstrated that ANGPTL4 may serve as a potential therapeutic target for cardiovascular diseases. The carriers of the E40K mutation in ANGPTL4 or other loss-of-function variants have lower levels of triglycerides and a reduced risk of coronary artery disease (CAD) [30, 31].Studies have reported that plasma ANGPTL4 levels can predict future cardiovascular events, indicating its potential as a biomarker for CAD. Similarly, research has shown that the serum levels of ANGPTL4 in T2DM patients are twice as high as in normal controls and are positively correlated with age [32]. This is consistent with our findings. We observed increased expression of ANGPTL4 in both the mouse DCM model and the cardiomyocytes model induced by glucose and lipid toxicity, and knockdown of ANGPTL4 improved the senescence phenotype of cardiomyocytes (Fig. 5), indicating that

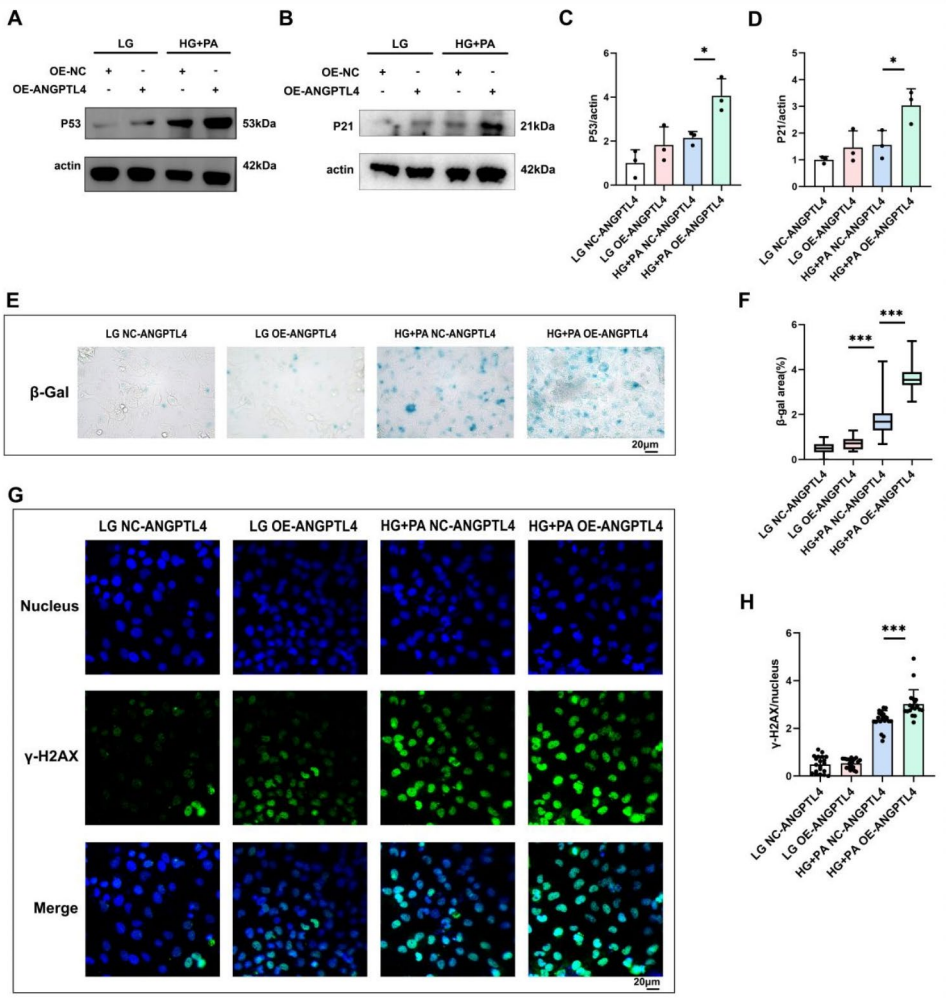

Fig. 6 Overexpression of ANGPTL4 Exacerbates HG + PA-Induced Cellular senescence in cardiomyocytes. (**A**-**D**) P53 and P21 proteins in cell lysates were detected by Western blotting. (**E** and **F**) β-gal staining of treated AC16 cells; scale bar, 20 mm. (**G** and **H**) Immunofluorescent staining of γ-H2AX (green) in treated AC16 cells; scale bar, 20 mm. Data are presented as mean ± SEM; *$p < 0.05$ **$p < 0.01$, ***$p < 0.001$

increased expression of ANGPTL4 plays a key role in the process of cardiomyocytes senescence.

To explore whether SGLT2i could improve cardiomyocytes senescence by targeting ANGPTL4, we overexpressed ANGPTL4 in the high glucose and high fat AC16 cell model (Fig. 7). The results showed that the addition of SGLT2i treatment significantly downregulated the expression of ANGPTL4 and cellular senescence-related markers. Previous studies have revealed an association between ANGPTL4 and SGLT2i, indicating that inhibiting SGLT2 can downregulate the expression of ANGPTL4 in adipose tissue, skeletal muscle, and the heart [33], but the specific mechanism has not been deeply investigated. Another important finding of our study is that SGLT2i directly affected the transcriptional level of ANGPTL4 in cardiomyocytes. Through literature review, we discovered a forkhead box transcription factor response element (FRE) in the promoter region of the ANGPTL4 gene, which is a binding site for FOXO1 [34]. FOXO1 is a transcription factor that plays a crucial role in regulating insulin signaling and cardiac metabolism. By modulating the expression of genes associated with glucose and lipid metabolism, such as through the influence on factors like SREBP-1c and PGC-1α, FOXO1 is involved in insulin action and resistance [35]. Studies have indicated that the expression of FOXO1 can be downregulated following the administration of SGLT2 inhibitors [36]. SGLT2 inhibitors may indirectly affect the FOXO1 signaling pathway by impacting metabolism in the kidney and heart, subsequently influencing glucose metabolism and inflammatory responses. Furthermore, SGLT2 inhibitors may mitigate the detrimental effects of FOXO1 in glucose and lipid metabolism by improving insulin sensitivity [37]. Similarly, in diabetes and diabetic cardiomyopathy, FOXO1 is overactivated in cardiomyocytes, which is associated with heart dysfunction

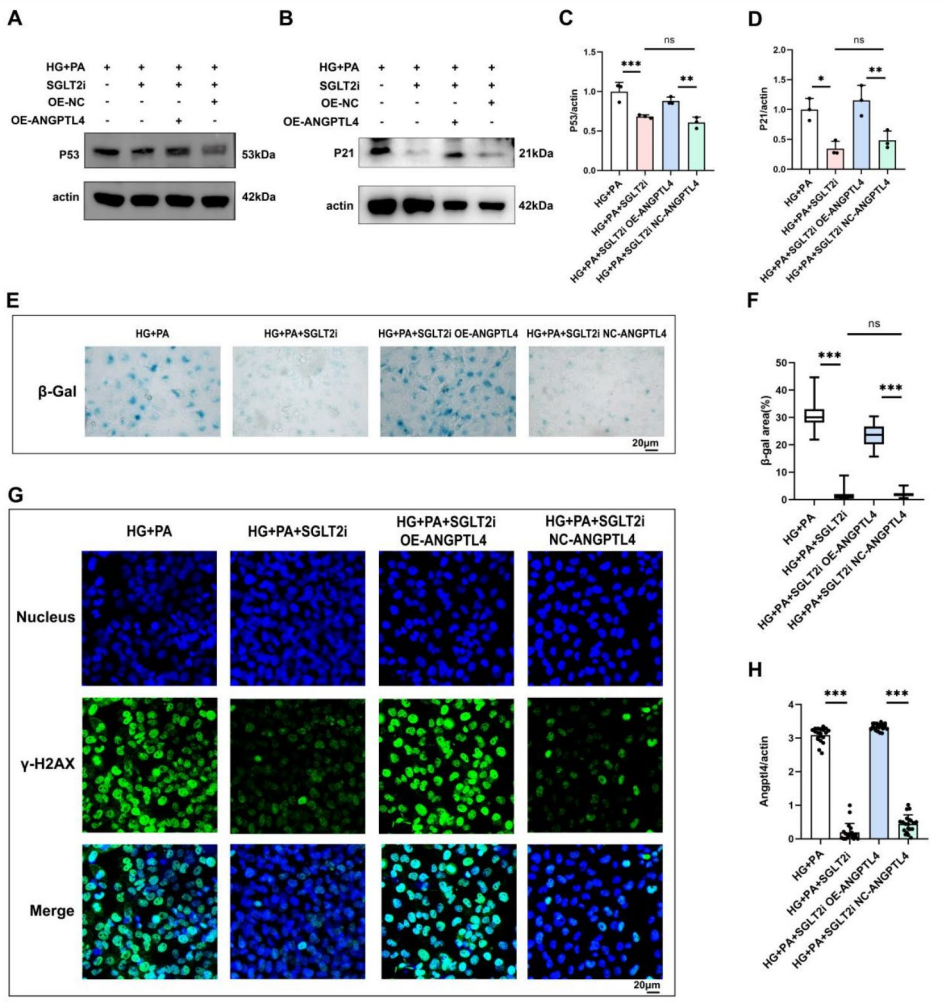

Fig. 7 SGLT2 inhibitors mitigate cellular senescence through ANGPTL4 modulation. **A**–**D** P53 and P21 proteins in cell lysates were detected by Western blotting. **E** and **F** β-gal staining of treated AC16 cells; scale bar, 20 mm. **G** and **H** Immunofluorescent staining of γ-H2AX (green) in treated AC16 cells; scale bar, 20 mm. Data are presented as mean ± SEM; $^{*}p < 0.05$ $^{**}p < 0.01$, $^{***}p < 0.001$

[38–40]. This is consistent with our results (Fig. 8). FOXO1 can bind to and promote the transcriptional synthesis of ANGPTL4, but in the treatment group, overexpression of FOXO1 did not increase the accumulation of ANGPTL4, indicating that SGLT2i, when administered, can directly affect the levels of ANGPTL4 in cardiomyocytes by reducing the pathway of FOXO1. This is the first report to elucidate the mechanism by which SGLT2i, through the FOXO1-ANGPTL4 pathway, confer anti-aging and protective effects at the cardiomyocytes level.

This study also has certain limitations. Firstly, we did not use an in vivo model in the investigation of the mechanism by which ANGPTL4 promotes cardiomyocytes senescence. The main reason is that approaches targeting ANGPTL4, which have been reported in previous literature, have been hindered due to the severe inflammatory effects observed in mice and monkeys [31, 41, 42]. Secondly, in our study, we did not utilize clinical human DCM samples. This limitation is compounded by the fact that there is no definitive gold standard for the clinical diagnosis of DCM, it can only be ascertained through a comprehensive assessment involving a suite of clinical evaluations and auxiliary tests. Moving forward, we intend to incorporate clinical samples in our research to bolster the external validity of our findings and to further substantiate our observations. Ultimately, in the Western blot experiments of this study, a full-length ANGPTL4 antibody was used, but the results showed the most significant difference in the expression of the C-terminal ANGPTL4. ANGPTL4 is a 50 kDa protein with a unique N-terminal helical-coil structural domain (nANGPTL4) of about 15 kDa and a C-terminal fibrinogen-like structural domain (cANGPTL4) of about 35 kDa, each domain undertaking different functions and being prone to dissociation. Literature has shown that ANGPTL4 promotes the occurrence of diabetic cardiomyopathy

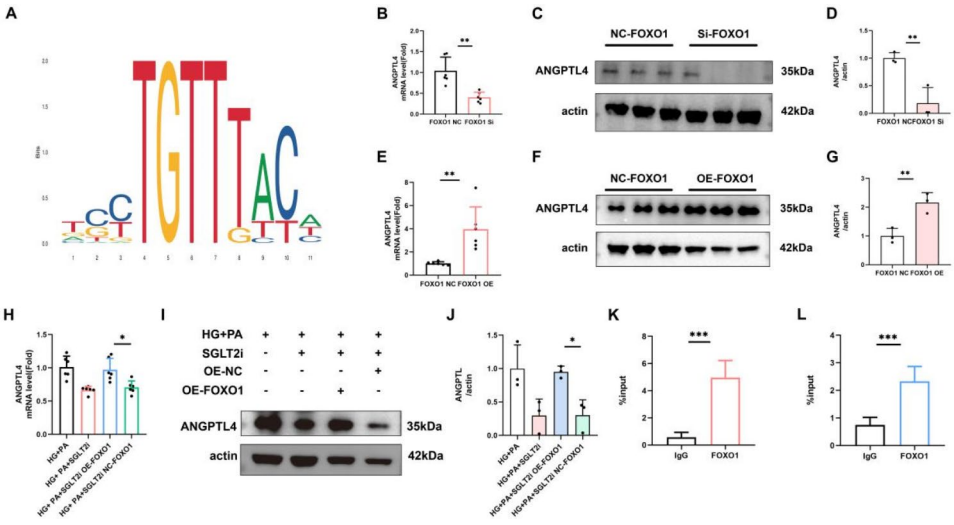

Fig. 8 SGLT2 Inhibitors Can Suppress the Transcription of ANGPTL4 by Reducing Cardiac FOXO1. **A** Expression of FOXO1 binding sites in the JASPAR database. **B**–**D** AC16 cells were transfected with FOXO1 siRNA (0.5μM) and incubated for 24 and 48 h, respectively, to detect the levels of ANGPTL4 mRNA and its protein. **E**–**G** AC16 cells were transfected with an overexpression plasmid of FOXO1 (2 μg/μl) and incubated for 24 and 48 h, respectively, to detect the levels of ANGPTL4 mRNA and its protein. **H**–**J** AC16 cells were treated with HG (33.3mmol/L) + PA (100μM) for 48 h, then transfected with an overexpression plasmid of FOXO1 (2 μg/μl) using lipo2000, followed by incubation with SGLT2 inhibitors (0.5μM) for an additional 48 h to detect the levels of ANGPTL4 mRNA and its protein. **K** Chromatin immunoprecipitation assay using AC16 cells to verify the binding sites of FOXO1 in the promoter region of ANGPTL4. **L** Chromatin immunoprecipitation assay using primary mouse cardiomyocytes to verify the binding sites of FOXO1 in the promoter region of ANGPTL4 Data are presented as mean ± SEM; *$p < 0.05$ **$p < 0.01$, ***$p < 0.001$

through integrin/oxidative stress pathways [43], which is the function of the cANGPTL4 domain, consistent with the results of this experiment. Further elucidation of the roles of different structural domains of ANGPTL4 in DCM is also a direction for our future research.

Conclusions

In summary, our study has discovered a new therapeutic mechanism of SGLT2i for cardiac protection, which is to regulate the binding of FOXO1 with ANGPTL4, inhibit the transcriptional synthesis of the latter, thereby improving the senescence of DCM cardiomyocytes induced by hyperglycemia and hyperlipidemia, and restoring cardiac function. Our research complements the mechanisms of action of SGLT2i in anti-aging and cardiac protection. In addition, we also see the potential application of therapeutic strategies targeting molecules such as FOXO1 and ANGPTL4, and further clinical translation is needed to assess their efficacy and safety.

Supplementary Information

The online version contains supplementary material available at https://doi.org/10.1186/s12933-024-02520-8.

Supplementary Material 1

Supplementary Material 1

Supplementary Material 1

Author contributions

LH.W and XF.Z contributed to study design. Y.W, XF.Z and H.L participated in the drafting of the article. Y.W, HW.Y, RX.W, JX.W, X.Y, MX.Y and Y.Wang carried out the experiments. Y.W, TQ.D and CX.M contributed to data collection and analysis. LY.W and YT.Z contributed to the literature search. All authors reviewed the manuscript.

Funding

This study was supported by Talent introduction funding project of the First Affiliated Hospital of Jinan University (No. 808026), National Natural Science Foundation of China (Grant Number: 82200417) and Funding by Science and Technology Projects in Guangzhou(2023A04J1280).

Data availability

No datasets were generated or analysed during the current study.

Declarations

Ethics approval and consent to participate

Jinan University Experimental Animal Welfare Ethics Committee approved all animal experiments in this study (IACUC-20220512-06).

Competing interests

The authors declare no competing interests.

Author details

[1]Department of Endocrinology and Metabolism, First Affiliated Hospital of Jinan University, Guangzhou, China
[2]The Academician Cooperative Laboratory of Basic and Translational Research on Chronic Diseases, The First Affiliated Hospital, Jinan University, Guangzhou, China
[3]Guangzhou Key Laboratory of Basic and Translational Research on Chronic Diseases, Jinan University, Guangzhou, China

Received: 16 October 2024 / Accepted: 20 November 2024
Published online: 04 December 2024

References

1. Mehdizadeh M, Aguilar M, Thorin E, Ferbeyre G, Nattel S. The role of cellular senescence in cardiac disease: basic biology and clinical relevance. Nat Rev Cardiol. 2022;19(4):250–64.
2. Hughes MJ, McGettrick HM, Sapey E. Shared mechanisms of multimorbidity in COPD, atherosclerosis and type-2 diabetes: the neutrophil as a potential inflammatory target. Eur Respir Rev. 2020;29(155):190102.
3. Henson SM, Aksentijevic D. Senescence and type 2 diabetic cardiomyopathy: how young can you die of old age. Front Pharmacol. 2021;12:716517.
4. Zhang Y, Zheng Y, Wang S, et al. Single-nucleus transcriptomics reveals a gatekeeper role for FOXP1 in primate cardiac aging. Protein Cell. 2023;14(4):279–93.
5. Chen MS, Lee RT, Garbern JC. Senescence mechanisms and targets in the heart. Cardiovasc Res. 2022;118(5):1173–87.
6. Kennedy BK, Berger SL, Brunet A, et al. Geroscience: linking aging to chronic disease. Cell. 2014;159(4):709–13.
7. Minamino T, Orimo M, Shimizu I, et al. A crucial role for adipose tissue p53 in the regulation of insulin resistance. Nat Med. 2009;15(9):1082–7.
8. Fontana L, Mitchell SE, Wang B, et al. The effects of graded caloric restriction: XII. Comparison of mouse to human impact on cellular senescence in the colon. Aging Cell. 2018;17(3):e12746.
9. Guo S, Deng W, Xing C, Zhou Y, Ning M, Lo EH. Effects of aging, hypertension and diabetes on the mouse brain and heart vasculomes. Neurobiol Dis. 2019;126:117–23.
10. Zhang X, Liu C, Liu C, Wang Y, Zhang W, Xing Y. Trimetazidine and l–carnitine prevent heart aging and cardiac metabolic impairment in rats via regulating cardiac metabolic substrates. Exp Gerontol. 2019;119:120–7.
11. Dillmann WH. Diabetic cardiomyopathy. Circ Res. 2019;124(8):1160–2.
12. Jia G, Hill MA, Sowers JR. Diabetic cardiomyopathy: an update of mechanisms contributing to this clinical entity. Circ Res. 2018;122(4):624–38.
13. Rådholm K, Figtree G, Perkovic V, et al. Canagliflozin and heart failure in type 2 diabetes Mellitus: results from the CANVAS program. Circulation. 2018;138(5):458–68.
14. Sattar N, McLaren J, Kristensen SL, Preiss D, McMurray JJ. SGLT2 inhibition and cardiovascular events: why did EMPA-REG outcomes surprise and what were the likely mechanisms. Diabetologia. 2016;59(7):1333–9.
15. Kaplinsky E. DAPA-HF trial: dapagliflozin evolves from a glucose-lowering agent to a therapy for heart failure. Drugs Context. 2020;9:2019–11.
16. Kulkarni AS, Aleksic S, Berger DM, Sierra F, Kuchel GA, Barzilai N. Geroscience-guided repurposing of FDA-approved drugs to target aging: a proposed process and prioritization. Aging Cell. 2022;21(4):e13596.
17. Hasan R, Lasker S, Hasan A, et al. Canagliflozin attenuates isoprenaline-induced cardiac oxidative stress by stimulating multiple antioxidant and anti-inflammatory signaling pathways. Sci Rep. 2020;10(1):14459.
18. Ndibalema AR, Kabuye D, Wen S, Li L, Li X, Fan Q. Empagliflozin protects against proximal renal tubular cell Injury Induced by high glucose via regulation of Hypoxia-Inducible factor 1-Alpha. Diabetes Metab Syndr Obes. 2020;13:1953–67.
19. Li C, Zhang J, Xue M, et al. SGLT2 inhibition with empagliflozin attenuates myocardial oxidative stress and fibrosis in diabetic mice heart. Cardiovasc Diabetol. 2019;18(1):15.
20. Klimontov VV, Korbut AI, Taskaeva IS, et al. Empagliflozin alleviates podocytopathy and enhances glomerular nephrin expression in db/db diabetic mice. World J Diabetes. 2020;11(12):596–610.
21. Gallo LA, Ward MS, Fotheringham AK, et al. Once daily administration of the SGLT2 inhibitor, empagliflozin, attenuates markers of renal fibrosis without improving albuminuria in diabetic db/db mice. Sci Rep. 2016;6:26428.
22. Neal B, Perkovic V, Mahaffey KW, et al. Canagliflozin and cardiovascular and renal events in type 2 diabetes. N Engl J Med. 2017;377(7):644–57.
23. Gao YM, Feng ST, Wen Y, Tang TT, Wang B, Liu BC. Cardiorenal protection of SGLT2 inhibitors-perspectives from metabolic reprogramming. EBioMedicine. 2022;83:104215.
24. Hoong C, Chua M. SGLT2 inhibitors as calorie restriction mimetics: insights on Longevity pathways and age-related diseases. Endocrinology. 2021;162(8):bqab079.
25. Mazzieri A, Basta G, Calafiore R, Luca G. GLP-1 RAs and SGLT2i: two antidiabetic agents associated with immune and inflammation modulatory properties through the common AMPK pathway. Front Immunol. 2023;14:1163288.
26. Mattison JA, Roth GS, Beasley TM, et al. Impact of caloric restriction on health and survival in rhesus monkeys from the NIA study. Nature. 2012;489(7415):318–21.
27. Kraus WE, Bhapkar M, Huffman KM, et al. 2 years of calorie restriction and cardiometabolic risk (CALERIE): exploratory outcomes of a multicentre, phase 2, randomised controlled trial. Lancet Diabetes Endocrinol. 2019;7(9):673–83.
28. Katsuumi G, Shimizu I, Suda M et al. SGLT2 inhibition eliminates senescent cells and alleviates pathological aging. Nat Aging. 2024.
29. Long J, Ren Z, Duan Y et al. Empagliflozin rescues lifespan and liver senescence in naturally aged mice. Geroscience. 2024.
30. Myocardial Infarction Genetics and CARDIoGRAM Exome Consortia Investigators, Stitziel NO, et al. Coding variation in ANGPTL4, LPL, and SVEP1 and the risk of coronary disease. N Engl J Med. 2016;374(12):1134–44.
31. Dewey FE, Gusarova V, O'Dushlaine C, et al. Inactivating variants in ANGPTL4 and risk of coronary artery disease. N Engl J Med. 2016;374(12):1123–33.
32. Aryal B, Price NL, Suarez Y, Fernández-Hernando C. ANGPTL4 in metabolic and cardiovascular disease. Trends Mol Med. 2019;25(8):723–34.
33. Basu D, Huggins LA, Scerbo D, et al. Mechanism of increased LDL (low-Density lipoprotein) and decreased triglycerides with SGLT2 (sodium-Glucose cotransporter 2) inhibition. Arterioscler Thromb Vasc Biol. 2018;38(9):2207–16.
34. Kuo T, Chen TC, Yan S, et al. Repression of glucocorticoid-stimulated angiopoietin-like 4 gene transcription by insulin. J Lipid Res. 2014;55(5):919–28.
35. Sajan MP, Lee MC, Foufelle F, Sajan J, Cleland C, Farese RV. Coordinated regulation of hepatic FoxO1, PGC-1α and SREBP-1c facilitates insulin action and resistance. Cell Signal. 2018;43:62–70.
36. Bamba R, Okamura T, Hashimoto Y, et al. Extracellular lipidome change by an SGLT2 inhibitor, luseogliflozin, contributes to prevent skeletal muscle atrophy in db/db mice. J Cachexia Sarcopenia Muscle. 2022;13(1):574–88.
37. Vallon V. State-of-the-Art-Review: mechanisms of action of SGLT2 inhibitors and clinical implications. Am J Hypertens. 2024;37(11):841–52.
38. Joubert M, Jagu B, Montaigne D, et al. The sodium-glucose cotransporter 2 inhibitor Dapagliflozin prevents cardiomyopathy in a Diabetic Lipodystrophic Mouse Model. Diabetes. 2017;66(4):1030–40.
39. Battiprolu PK, Hojayev B, Jiang N, et al. Metabolic stress-induced activation of FoxO1 triggers diabetic cardiomyopathy in mice. J Clin Invest. 2012;122(3):1109–18.
40. Qi Y, Zhu Q, Zhang K, et al. Activation of Foxo1 by insulin resistance promotes cardiac dysfunction and β-myosin heavy chain gene expression. Circ Heart Fail. 2015;8(1):198–208.
41. Aryal B, Rotllan N, Araldi E, et al. ANGPTL4 deficiency in haematopoietic cells promotes monocyte expansion and atherosclerosis progression. Nat Commun. 2016;7:12313.
42. Landfors F, Henneman P, Chorell E, Nilsson SK, Kersten S. Drug-target mendelian randomization analysis supports lowering plasma ANGPTL3, ANGPTL4, and APOC3 levels as strategies for reducing cardiovascular disease risk. Eur Heart J Open. 2024;4(3):oeae035.
43. Dai L, Xie Y, Zhang W, et al. Weighted gene co-expression network analysis identifies ANGPTL4 as a key regulator in diabetic cardiomyopathy via FAK/SIRT3/ROS pathway in cardiomyocyte. Front Endocrinol (Lausanne). 2021;12:705154.

Publisher's note